Propagating wave pattern on a falling liquid curtain

N. Le Grand-Piteira,[1,2] P. Brunet,[1,*] L. Lebon,[1,2] and L. Limat[1,2]
[1]*Laboratoire de Physique et Mécanique des Milieux Hétérogènes, UMR 7636 CNRS, 10, rue Vauquelin, 75005 Paris, France*
[2]*Laboratoire Matière et Systèmes Complexes, UMR 7057 du CNRS, Université Paris 7, 2 place Jussieu, 75251 Paris Cedex 05, France*
(Received 10 August 2005; revised manuscript received 20 March 2006; published 22 August 2006)

A regular pattern of surface waves is observed on a liquid curtain falling from a horizontal, wetted tube, maintained between two vertical wires. Since the upper boundary is not constrained in the transverse direction, the top of the curtain enters a pendulumlike motion, when the flow rate is progressively reduced, coupled to the propagation of curtain undulations, structured as a checkerboard. This structure is formed by two patterns of propagating waves. In some sense, these propagating patterns replace the stationary pattern of liquid columns observed at a lower flow rate. Measurements of phase velocity, frequency, and wavelength are reported. The data are in agreement with a simple dimensional argument suggesting that the wave velocity is proportional to the surface tension divided by the mass flux of liquid per unit length. This scaling is also that followed by the fluid velocity at the so-called transonic point, i.e., the point where the fluid velocity equals that of sinuous waves. We finally discuss the implications of these results for the global stability of liquid curtains.

DOI: 10.1103/PhysRevE.74.026305 PACS number(s): 47.20.Ma, 47.54.−r

I. INTRODUCTION

Many studies have been devoted to the appearance and dynamics of organized structures in nonlinear dissipative spatially extended systems [1], especially in one space dimension [2]. These patterns have been observed in various physical systems such as, among others, hydro-thermal waves [3,4], Taylor-Dean instability [5], directional solidification [6], directional viscous fingering [7,8], and so on. They are important for the understanding of morphogenesis in general, and also in the context of transition to turbulence in hydrodynamics [9–11]. Roughly, one can distinguish two classes of phenomena. In the first class, the primary pattern is stationary, but dynamics can develop from secondary bifurcations linked to specific symmetry breaking [12]. In the second class, the primary pattern is propagative and drifts at a well-defined phase speed, the phenomenology of the dynamics being often well captured by complex Ginzburg-Landau equations [13].

Among the diverse investigated systems, one has recently received a special interest because of its simplicity and of the possibility to force at will initial conditions: when a liquid is falling continuously from a horizontal ceiling, regular lattices of liquid columns hanging below the ceiling are observed [14,15], and exhibit striking collective dynamics [16]. The dynamics of this pattern have motivated several studies in three different geometries: (i) liquid columns formed below a horizontal wetted tube [16,17], (ii) liquid columns formed below the perimeter of a overflowing dish [18–21], and (iii) two-dimensional (2D) lattices formed below a porous grid [22,23]. In each case, the pattern belongs to the first class, i.e., to the group of stationary primary patterns, and one may ask whether there could exist an equivalent of the second class of pattern for this kind of flow. In the present paper, we show that this equivalent indeed exists, but in a higher-flow-rate regime. When the liquid columns are replaced by a continuous liquid curtain extending over the whole ceiling, and in a specific range of flow rate, this curtain exhibits a pattern of sinuous waves, coupled with modulations of the film hanging below the ceiling, both perturbations propagating along the ceiling at constant speed.

The pattern of sinuous waves is reproduced in Fig. 1, the curtain being formed in the present paper below a uniformly wetted tube continuously supplied with liquid [16,17]. The

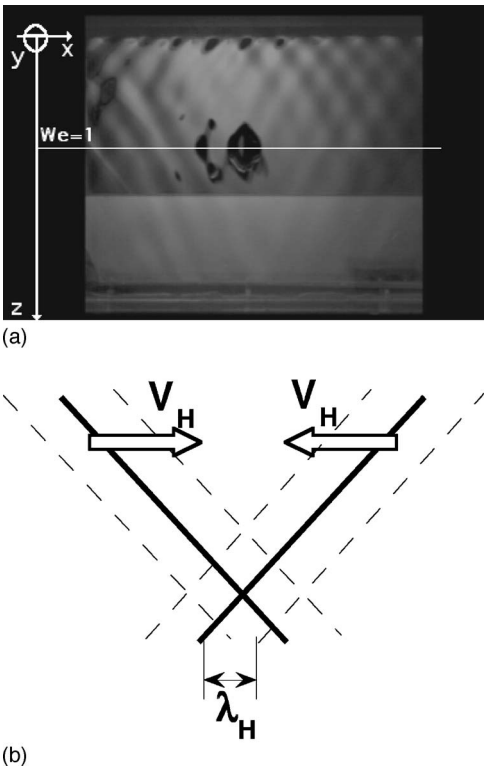

FIG. 1. (a) Checkerboard structure resulting from two sets of propagating waves on a liquid curtain. (b) Definition of the horizontal wave velocity V_H and wavelength λ_H.

*Present address: Department of Mathematics, University of Bristol, BS8 1TW Bristol, United Kingdom. Electronic address: brunet@mech.kth.se

lateral sides of the curtain are maintained vertical with two wires put under tension. Surprisingly, both sets of waves preserve their shape while propagating, i.e., they travel from one side to another at a speed independent of the vertical position z. This is remarkable, because such curtains are highly stretched by the acceleration of gravity, and thus both the fluid velocity and curtain thickness strongly vary with z, evolving, respectively, as $U^2 \simeq 2gz$ and $h=\Gamma/U \sim z^{-1/2}$. As a result, it could be expected that the velocity of the waves propagating along the curtain depends also on z. Let us recall that according to the available literature [24–31], two kinds of waves can propagate on a curtain: a symmetrical mode (varicose waves) corresponding to thickness modulations, and an antisymmetrical mode (sinuous mode) corresponding to modulations of the median transverse position of the curtain [24]. In the asymptotic conditions of a weak amplitude (linear approximation) and in the limit of an inviscid ambient gas, these waves have the following velocities:

$$c_{\mathrm{var}} = \sqrt{\frac{\gamma h}{2\rho}}k, \tag{1}$$

$$c_{\mathrm{sin}} = \sqrt{\frac{2\gamma}{\rho h}}, \tag{2}$$

which indeed depend on z through the curtain thickness $h(z)$.

Another surprise in this experiment is that these large-amplitude undulations extend on the whole curtain, including a large upstream domain (also denoted the "subsonic" domain in the following), in which the Weber number We is smaller than 1. Let us recall that $\mathrm{We}=\rho h U^2/2\gamma$ is built upon surface tension γ, liquid density ρ, local liquid velocity U, and local curtain thickness h. According to the available literature, it is predicted that the very existence of the domain $\mathrm{We}<1$ could lead to curtain rupture provided that the size of this upstream domain becomes large enough [30–32]. Indeed, in this case, sinuous waves are able to travel upstream against the flow, in the upstream domain [$\mathrm{We}<1$ implies that $U(z)<c_{\mathrm{sin}}$]. It is, however, worth mentioning that curtain stability criteria built upon wave amplification have been recently contested [33], and the present experiment is perhaps an observation in favor of this new point of view.

In this paper, we present an investigation of this pattern, and provide in particular measurements of its frequency, wavelength, and phase velocity, varying flow rate, liquid properties, and tube radius. We also suggest tentative scaling laws for these quantities, starting from simple dimensional and physical arguments. In particular, we suggest that the phase velocity could be proportional to the velocity of the fluid at the so-called transonic line of the curtain, i.e., at the horizontal line where the liquid velocity is exactly equal to that of sinuous waves. This line is also the location where $\mathrm{We}=1$, i.e., the separation line between the convective zone (downstream) and the absolute zone (upstream) for sinuous surface waves. Let us mention here that observations of spontaneous waves on a falling sheet, although possibly involving different mechanisms, have been reported very recently in other geometries, such as a liquid curtain falling across a flat horizontal grid [34] or attached below an overflowing circular dish [35]. This shows the great generality of this surprising pattern that should deserve in the future more extensive studies. A brief account of some of our early observations is available in Ref. [36].

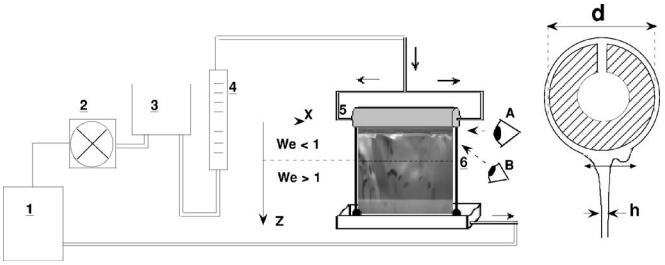

FIG. 2. Sketch of the experiment. The curtain, guided between two long vertical threads, falls from a horizontal uniformly wetted hollow tube. The liquid is supplied through a long thin slot drilled all along the tube and turned upward. On the right part of the figure, the flow structure viewed from position A is suggested. The picture reproduced in Fig. 5(a) is taken from position B.

The paper is organized as follows. In Sec. II, the experimental setup is described and typical scalings governing the flow are recalled. Section III presents our observations and data, as well as attempted scaling laws based on dimensional analysis, before the final discussion in Sec. IV.

II. EXPERIMENTAL CONDITIONS

A. Experimental setup

The experiment is suggested in Fig. 2. The liquid is extracted from a reservoir (1) by a gear pump ISMATEC BVP-Z (2) that imposes a constant flow rate Q. The flow rate is measured with a float flowmeter (4). A half-filled chamber (3) damps remaining perturbations. The liquid is injected at the two ends of a horizontal hollow tube (5) (diameter d equal to 3.4 and 6.8 cm), and flows on its external surface from a long thin slot (thickness $e=2$ mm) drilled on its upper side. If the flow rate is sufficiently high, a liquid curtain is observed (6). Its width ($w=25.5$ cm) is kept constant along the vertical direction by two thin nylon threads (diameter 0.01 cm) put under tension by two weights attached at their lower ends. These two vertical wires pin the edges of the curtain and thus they prevent the shrinkage caused by surface tension that would occur otherwise. The height of the curtain can be chosen from 15 to 25 cm, by tuning the vertical position of an intermediate tank. All the experiments are performed with silicon oils [polydimethylsiloxane (PDMS)], of viscosity ranging from 10 to 50 cP. Their physical properties are listed in Table I. The surface tension and density are

TABLE I. Physical properties of liquids.

Liquid reference	ν (mm^2/s)	γ (dyn/cm)	ρ (g/cm^3)
PDMS 47V10	10.3	20.1	0.935
PDMS47V30	32.0	20.4	0.947
PDMS47V50	53.6	20.7	0.957

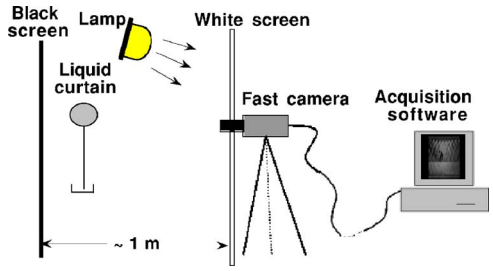

FIG. 3. (Color online) Principle of the visualization.

close for the three oils. In the following, the three liquids will be simply referred to as V10, V30, or V50. We have checked that the liquid lies at room temperature, which was between 20 and 22 °C during the experiments. Special care was taken to protect the system from any sources of perturbations, especially air stream from the atmosphere around the experiment.

Curtain undulations are followed by a high-speed video camera (FASTCAM 1024 Motion-Corder). In practice, a frequency of 250 images per second is sufficient to capture the phenomena under study. Because of the required short acquisition time, it is important to use a powerful and nonpulsed light source. Furthermore, the light diffused by the curtain has to be as homogeneous as possible. The chosen solution, depicted in Fig. 3, uses a 300 W incandescent lamp which lights a white screen, the latter diffusing a homogeneous light on the curtain. Another screen, black colored, is put behind the curtain, to maximize contrast. A circular hole is drilled through the white screen, in which the camera lens fits. The reflection of this hole induces a parasite round black shadow on the pictures, of very limited extent, which does not hinder quantitative measurements. The lateral edges are the nylon wires mentioned above.

In contrast with previous experiments on liquid curtains [25,26,28,31], our geometry allows lateral motions of the top of the curtain. Most of previous work involved curtains falling directly from a slot or from a sharp edge, which constrains the detachment line position. It is presumably why the checkerboard structure has never been reported in the available literature up to now, to our knowledge.

B. Description of the flow: Some helpful scalings

In this section, we discuss in more detail the flow structure involved in the curtain, and provide the readers with scalings that will help them to understand the measured data. The key control parameter of the experiment is the flow rate per unit length Γ, which is simply equal to the volumetric flow rate Q divided by the width of the curtain w. Typical values for Γ range between 0.1 and 2 cm^2/s.

In most studies on curtains, it is assumed and checked [26,29,37] that the flow structure is at first order a plug flow, i.e., that U is constant along the y direction providing that one measures sufficiently far from the slot, or more generally from the detachment point (typically more than a few millimeters away). The case of a curtain detaching directly from a slot (placed at $z=0$ in what follows) is perhaps the most well known. In his pioneering study, Brown [25] established a semiempirical law for the vertical velocity in the curtain, which is approximately given by $U^2=U_0^2+2g[z-2(4\nu)^{2/3}/g^{1/3}]$ where U_0 denotes the mean velocity of the flow across the slot, ν the kinematic viscosity, and g the acceleration of gravity. Our situation is not too different from that involved for a millimetric slot: U_0 does not exceed 10 mm/s, and the term U_0^2 should become negligible for z larger than $U_0^2/(2g) \simeq 0.05$ mm. Also, the offset on z given by the viscous corrective term is of order 0.3 mm, and should also become negligible downstream of this offset. Then, far enough from the bottom of the tube, the velocity field should simply reduce to a free-fall law:

$$U^2 = 2gz. \tag{3}$$

This assumption was checked by the method already described in [26,29,40], i.e., by measuring the opening angle of sinuous wakes left behind a needle touching the curtain. By analogy with the supersonic Mach cone, half the angle formed by the wake at its summit, θ, is related to the velocity of the flow U and $c_{\sin}$ by the relationship

$$\sin\theta = \frac{c_{\sin}}{U}. \tag{4}$$

The velocity $c_{\sin}$ is given by Eq. (2), which gives

$$c_{\sin} = \sqrt{\frac{2\gamma}{\rho h}} = \sqrt{\frac{2\gamma U}{\rho\Gamma}}. \tag{5}$$

Thus, one obtains

$$\sin\theta = \left(\frac{2\gamma}{\rho\Gamma}\right)^{1/2} U^{-1/2}. \tag{6}$$

In practice, a good agreement between Eq. (3) and measurements was obtained by taking the origin $z=0$ at the bottom of the cylinder [Fig. 1(a)], for any flow rate Γ we tested (from 1.2 to 2.2 cm^2/s). A typical example is given in Fig. 4: by measuring θ [Fig. 4(a)], we plot the quantity $(\Gamma^2 \sin^4\theta)^{-1}$ [equal to $(g\rho^2/2\gamma^2)z$ according to Eqs. (3) and (6)] versus z, the vertical position of the wet obstacle. The prefactor $g\rho^2/2\gamma^2$ equals 1.05 for our parameters, which is in agreement with the data. Thus Eq. (3) can be considered as valid in the range of parameters of the study. This velocity profile suggests that the initial momentum at the top of the curtain is small compared to the momentum supplied to the liquid by gravity forces. It also implies that the local properties of the curtain (the thickness, the speed of surface waves, and so on) are very dependent on z: the curtain is clearly a nonparallel flow.

Furthermore, what is mentioned above has implications for the location of the singular point We=1 on the curtain. The length of the subsonic area, which equals the vertical position z^* where We=1, is tuned by Γ. It obeys the following relationship:

$$\mathrm{We} = \frac{\rho\Gamma(2gz^*)^{1/2}}{2\gamma} = 1, \tag{7}$$

which leads to

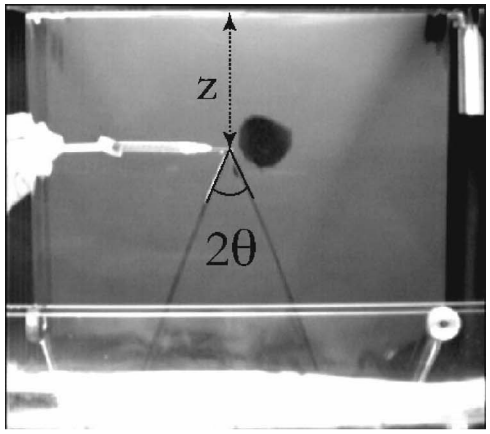

(a)

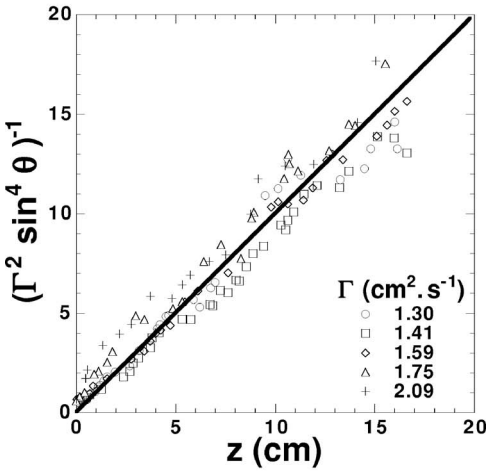

(b)

FIG. 4. (a) A typical sinuous wake formed by a needle soaked in the curtain. (b) Check of the free-fall law with no offset at the origin $U^2=2gz$ (continuous line) for several flow-rate values (silicon oil V50, cylinder diameter $d=4.7$ cm).

$$z^* = \frac{2\gamma}{g\rho^2\Gamma^2}. \tag{8}$$

The Weber number increases as z increases downstream and it is smaller than 1 when $z<z^*$. This property enables a useful method for locating the transonic line: this is the location where the sinuous wake below an obstacle vanishes when moving the obstacle upstream [28]. Note that, as any change on Γ modifies the liquid thickness in the whole curtain without modifing the velocity field, an increase of Γ leads to increase *everywhere* in the Weber number.

III. THE CHECKERBOARD WAVE PATTERN

A. General qualitative features

Experiments are developed as follows. First, a curtain is obtained by setting Γ at a very high value (typically 5 cm^2/s). The lateral nylon wires are then put in contact with the curtain lateral boundaries, which get pinned on them. The wires are then relaxed toward the vertical direction. Afterward the flow rate is progressively decreased until the two sets of waves appear. The subsequent checkerboard structure covers the whole curtain, including the downstream area where $We \geqslant 1$ [Fig. 1(a)]. We have observed that the wave velocity, measured horizontally and denoted V_H [defined in Fig. 1(b)] is nearly independent of z. The two sets of waves propagate toward opposite directions and do not seem to interact. Instead, they cross each other and get superimposed. Furthermore, neither waves seems to "see" the curtain edges and in particular they are not reflected on them. Therefore, although a uniform wavelength is seemingly selected on the whole pattern, it is not selected by the width of the curtain: The wavelength does not need to be a subdivision of this width.

As suggested by the right part of Fig. 2, this pattern appears in coincidence with a pendulumlike motion of the top of the curtain along its transverse direction, coupled with the transient appearance of "bulges" on the film flowing below the cylinder. Presumably, these bulges are formed by the Rayleigh-Taylor instability [17] and sustain the curtain oscillations by successive appearance and merging with the curtain. This mechanism is reminiscent of that sometimes invoked to explain oscillations of the network of liquid columns replacing the curtain at low flow rate [18], and supports the idea that in some sense the sets of propagating waves can be viewed as a drifting equivalent of the stationary pattern of liquid columns.

The pendulum motion of the curtain has been evidenced by views of the cylinder taken from below (direction B suggested in Fig. 2), a typical example being available in Fig. 5(a). The detachment position y_0 varies along the x axis, which leads to a sinuous "snake" structure on top of the curtain, when the two sets of spatially periodic and propagative waves are created. This observation is also a sign of the sinuous nature of the involved waves.

B. Measurements of checkerboard properties: Phase velocity

Measurements are achieved in the following way. Gray levels are extracted along a horizontal line recorded at a distance between 1 and 2 cm below the tube, from images of the curtain such as that shown in Fig. 1(a). By recording these gray levels at successive time steps, one obtains a spatiotemporal diagram from which V_H, f, and λ can be extracted [Fig. 5(b)]. The wave velocity $V_H=\Delta X/\Delta t$, frequency $f=1/T$, and wavelength λ_H are directly obtained from these diagrams. Measurements extracted from different vertical locations $z=$const on the curtain did not show any variations of those quantities, and the chosen location was just the one that provided the best contrast.

Measurements of V_H versus flow rate per unit length Γ are plotted in Fig. 6(a), for three viscosity values and for two different tube diameters. It turns out that at first order ν (kinematic viscosity) and d (tube diameter) do not influence the velocity of the waves, although they play a role in the range of existence of the pattern (see later in the text). A sharp increase of the speed is noticeable when Γ is decreased below 0.8 cm^2/s. The quantity $\gamma/(\rho\Gamma)$ is plotted in Fig. 6(a) (dotted line), and it turns out that this quantity fits very well the measured values of V_H.

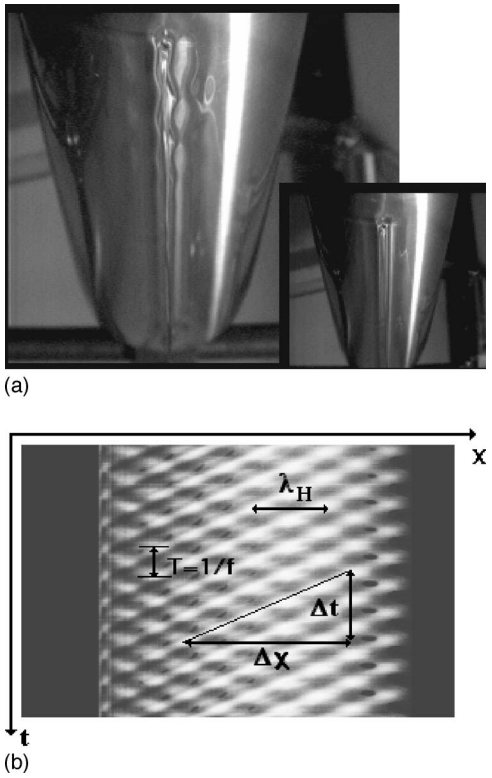

FIG. 5. (a) A curtain with the checkerboard structure, viewed from below, at 45° from the vertical (B direction in Fig. 2). Right inset: a similar view of the curtain without the waves. (b) Spatiotemporal diagram of the two patterns of waves.

The choice for this velocity can be justified with a simple physical argument using dimensional analysis. Basically the curtain undulations are traveling under the combined actions of two velocities, the fluid velocity $U=(2gz)^{1/2}$ and that of sinuous waves that reads $c_{\sin}=\sqrt{2\gamma/\rho h}=\sqrt{2\gamma U/\rho\Gamma}$. As V_H does not depend on z, it should be a combination of these two velocities that would be independent of z. The sole suitable combination reads therefore

$$\frac{c_{\sin}^2}{U}=\frac{2\gamma}{\rho\Gamma}\sim V_H\simeq\frac{\gamma}{\rho\Gamma}. \tag{9}$$

It is also worthwhile to notice that $V_H\sim\gamma/(\rho\Gamma)$ is half the speed of the sinuous waves at the transonic line (i.e., the line where We=1). This suggests that this line could play an essential role in the selection of the pattern velocity. It is, however, important to note that despite this selection, the pattern does not exhibit any discontinuity at the transonic line and looks similar in both subsonic and supersonic zones (see Fig. 1). Furthermore, even though the flow is highly nonparallel, the wave crests are only slightly curved and the pattern does not vary a lot along z. This is a bit surprising: U scales as $\sim z^{1/2}$, h scales as $\sim z^{-1/2}$, and $c_{\sin}$ scales as $\sim z^{1/4}$, which would have *a priori* suggested a dramatic change in the shape of the wave crests on approaching $z=0$, at least from a linear point of view. This means that the pattern velocity, and also presumably the frequency and the wavelength, are global properties of the pattern resulting from a nonlinear selection process. We discuss implications of this point in the Conclusion.

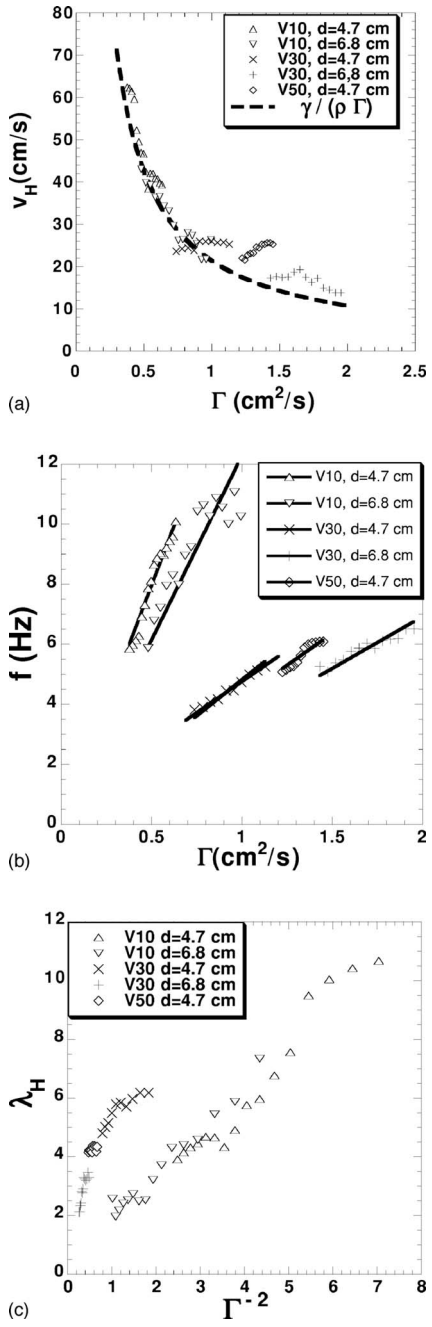

FIG. 6. (a) Velocity of the traveling waves V_H plotted versus flow rate Γ for different viscosities and cylinder diameters. The superimposed dashed curve is the typical velocity $\gamma/(\rho\Gamma)$, calculated with $\rho\simeq 20.3$ dyn/cm and $\rho\simeq 0.95$ g/cm^3 (see text). (b), (c) Same plots for the pattern frequency f versus Γ and for the wavelength versus $1/\Gamma^2$. The lines are linear fits crossing the origin.

C. Measurements of checkerboard properties: Frequency and wavelength

If one now still keeps in mind the simple idea that the pattern properties are selected at the transonic line, one

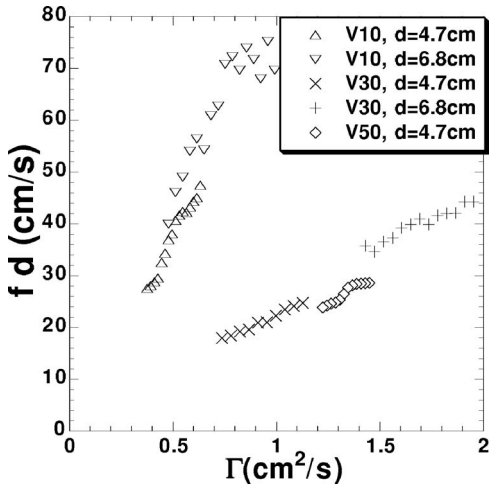

FIG. 7. Typical transverse curtain velocity fd versus Γ.

should expect a pattern wavelength scaling as $\lambda \sim z^* = 2\gamma/(g\rho^2\Gamma^2)$ and a frequency given by $f = V_H/\lambda \sim \rho g \Gamma/\gamma$. Both quantities are plotted in Figs. 6(b) and 6(c). As expected f seems to be proportional to Γ, while λ scales as $1/\Gamma^2$ (at least for the smaller viscosity), but both quantities involve prefactors that depend on d and ν. Roughly, f decreases with both increasing liquid viscosity ν and increasing tube radius d, while the dependence is the opposite for λ. This is in contrast with the wave velocity V_H, which did not depend on these two quantities, or was at least weakly dependent.

Despite several attempts, we were unable to find a simple scaling for both f and λ combining both the liquid viscosity and the tube diameter. It is particularly important to note that the data obtained for V30 and V50 oils are very close despite a ratio of viscosities equal to 5/3. On the other hand, complementary measurements (not reported here) convinced us that the frequency was inversely proportional to the tube diameter for centimetric tubes. Though only two tube diameters are here available, this can be made visible by plotting the velocity fd versus Γ, the obtained graph being reproduced in Fig. 7. As one can judge from these pictures, all the data collapse on at most two branches, each of these being possibly associated with respectively, low and high viscosities, but this point remains to be investigated in more detail. For the moment, we do not know the physical origin of the dependence on d. A possible idea here is that the typical transverse velocity of the curtain, which scales as fd, could be driven by the velocity of the liquid flowing below the tube, in a domain where the film thickness is not governed by the lubrication approximation but rather saturates to a constant value (capillary length, for instance).

Finally, these plots also contain information on the range of existence of the wave pattern, which depends on both ν and d: for a given ν, the use of a larger cylinder diameter d shifts the range of existence to higher flow rates. If d is fixed and ν is varied, the range of existence seems to be shifted to higher Γ at higher ν (although it is less obvious than the influence of d). For the V50 oil, the range is reduced: this is due to the fact that, when the flow rate is decreased below a critical value, the curtain can separate into two parallel thinner curtains, localized symmetrically to each other from the median plane (yOz), as shown in Fig. 8. Consequently, it is not possible to observe the wave pattern with the largest diameter used in this experiment ($d=6.8$ cm) and the V50 oil. For high viscosities, the curtain existence range is reduced because of such a separation: considering the pendulum motion of the curtain, this situation occurs when the allowed spatial range for the curtain detachment is too large.

IV. DISCUSSION AND CONCLUSIONS

This study reports a further curtain instability leading to a pattern of propagative waves. This pattern involves pendulumlike oscillations of the top of the curtain. These oscillations are enabled by the use of a smooth overhang which provides unconstrained boundary conditions. Thus, one can determine that conditions for this instability are twofold. First, the subsonic area has to be large enough to enable the growth of perturbations generated in the vicinity of the transonic point. Second, the inlet should allow for the perturbations to be reflected on top, which is enabled by the free-constrained conditions in the transverse direction. This pattern is observed when the flow rate is progressively decreased below a threshold (not studied in detail here), while remaining above curtain rupture. This is reminiscent of recent observations of oscillating annular liquid sheets (liquid bells) formed below an overflowing dish or a porous ring [34,35].

Even if the hydrodynamic mechanisms for velocity and frequency selections still need to be more clearly understood, the measurements reported here provide several clues.

(1) The wave velocity is related to the properties of the transonic line $(z=z^*)$: its absolute value is half the liquid speed at z^* (which also equals half the sinuous wave speed at z^*), and does not depend on the vertical location on the curtain. This fact puts into evidence that the selection mechanism involves properties of the transonic line, which is also the physical boundary where sinuous waves turn from convectively to absolutely unstable. The wave speed of the pattern does not depend on ν or d either, or is at most weakly dependent.

(2) The frequency measurements exhibit a linear dependence on flow rate. The frequency also depends on ν and d, and presumably on other parameters like the surface tension and the density of the liquid. All these parameters should influence the complex shape of the free surface just below the overhang, which may be involved in the wavelength and the frequency selection.

Furthermore, some points of our study can be related to the still disputed problems of curtain stability and that of the physical mechanisms leading to the breakup. In particular, our observations show that sinuous waves, which are sometimes invoked to explain curtain breakup [27,29,30,39], can be withstood at relatively high amplitudes without breakup. This fact underlines the discrepancy between linear theories that predict the curtain breakup by wave amplification [27,29,39], and experimental situations where an entirely subsonic curtain can be observed without breakup [28,36,40]. This point has been theoretically reconsidered in

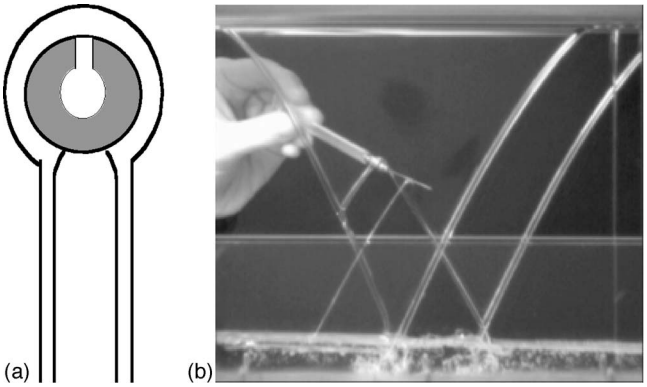

FIG. 8. For big tubes, the curtain can split into two parallel thiner ones. $d=6.8$ cm, V50, $\Gamma=1.95$ cm^2/s. The wake induced by curtain rupture below a needle helps here to visualize the coexistence of the two thin curtains. In this situation, the curtains cannot become pinned on the vertical wires at the edges, and the curtains shrink downstream.

a recent paper [33], which suggests that even when sinuous waves lead to the appearance of a global unstable mode in the whole curtain, rupture could be delayed because they involve the thinning of the sheet at molecular thickness. We suggest that the checkerboard structure could be the outward sign of a global mode, if one considers its spatial homogeneity and its strong selection mechanism. In the framework of convective or absolute instabilities of weakly nonparallel flows, it is predicted [38] that a global mode may appear when the length of the area of absolute instability (in the curtain, the area $\mathrm{We}\leqslant 1$) is larger than a certain threshold. The decrease of flow rate indeed leads to the extension of the area where $\mathrm{We}\leqslant 1$, and this could explain why the pattern is only observed below a certain flow-rate threshold.

This study finally illustrates the influence of the modification of the upper boundary conditions on the dynamics and stability of liquid curtains. In some sense, the configuration of the present study is perhaps more "natural" to capture intrinsic properties of the curtain than the usual configuration using an injection slot, which adds a constraint at the top of the curtain. Qualitatively, we have also begun to investigate the influence of the bottom boundary of the curtain. Surprisingly, one can maintain curtains at very low flow rates by adding a thin cylinder (of typical radius less than 0.5 cm) at the bottom of the curtain [36]. Such a situation is suggested in Fig. 9, where appearance of a black film and of rainbow patterns bear witness that the local thickness can be of order of the light wavelength without breaking. Local perturbations on such thin curtains (caused by a soaked obstacle, for example) do not necessary lead to breakup [41]. This surprising effect is presently under study.

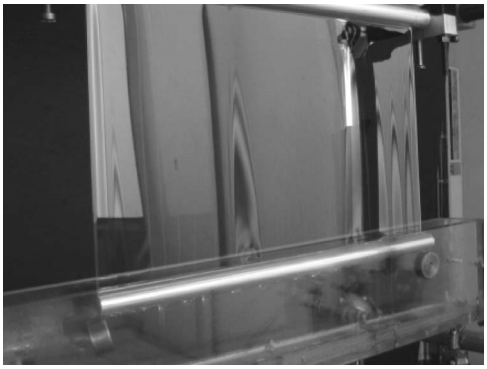

FIG. 9. An ultrathin curtain obtained with a bottom boundary condition constrained by a horizontal tube attached to the guides. Several rainbow patterns are observed ($\Gamma=0.015$ cm^2/s, V30 oil).

ACKNOWLEDGMENTS

We are indebted to Y. Bourremel, A. Renaud, and J.-S. Roche for complementary experiments.

[1] M. C. Cross and P. C. Hohenberg, Rev. Mod. Phys. **65**, 851 (1993).
[2] J.-M. Flesselles, A. J. Simon, and A. J. Libchaber, Adv. Phys. **40**, 1 (1991).
[3] N. Garnier and A. Chiffaudel, Phys. Rev. Lett. **86**, 75 (2001).
[4] J. Burguete, N. Mukolobwiez, F. Daviaud, N. Garnier, and A. Chiffaudel, Phys. Fluids **13**, 2773 (2001).
[5] P. Bot and I. Mutabazzi, Eur. Phys. J. B **13**, 141 (2000).
[6] A. J. Simon, J. Bechhoefer, and A. Libchaber, Phys. Rev. Lett. **61**, 2574 (1988).
[7] H. Z. Cummins, L. Fourtune, and M. Rabaud, Phys. Rev. E **47**, 1727 (1993).
[8] L. Pan and J. R. de Bruyn, Phys. Rev. Lett. **70**, 1791 (1993).
[9] A. Prigent, G. Gregoire, H. Chaté, O. Dauchot, and W. van Saarloos, Phys. Rev. Lett. **89**, 014501 (2002).
[10] D. Barkley and L. S. Tuckerman, Phys. Rev. Lett. **94**, 014502 (2005).
[11] R. Kerswell, Nonlinearity **18**, R17 (2005).
[12] P. Coullet and G. Iooss, Phys. Rev. Lett. **64**, 866 (1990).
[13] J. Burguete, H. Chaté, F. Daviaud, and N. Mukolobwiez, Phys. Rev. Lett. **82**, 3252 (1999).
[14] G. M. Carlomagno, in Proceedings of the Second AIMETA Congress 1974, Napoli, Italy, p. 253.
[15] W. G. Pritchard, J. Fluid Mech. **165**, 433 (1986).
[16] F. Giorgiutti, A. Bleton, L. Limat, and J. E. Wesfreid, Phys. Rev. Lett. **74**, 538 (1995).
[17] L. Limat, P. Jenffer, B. Dagens, E. Touron, M. Fermigier, and J. E. Wesfreid, Physica D **61**, 166 (1992).
[18] F. Giorgiutti and L. Limat, Physica D **103**, 590 (1997).
[19] C. Counillon, L. Daudet, T. Podgorski, M. C. Jullien, S. Akamatsu, and L. Limat, Europhys. Lett. **40**, 37 (1997).
[20] P. Brunet, J.-M. Flesselles, and L. Limat, Europhys. Lett. **56**, 221 (2001).
[21] P. Brunet and L. Limat, Phys. Rev. E **70**, 046207 (2004).

[22] P. Brunet, G. Gauthier, L. Limat, and D. Vallet, Exp. Fluids **37**, 645 (2004).
[23] C. Pirat, C. Mathis, P. Maissa, and L. Gil, Phys. Rev. Lett. **92**, 104501 (2004).
[24] G. I. Taylor, Proc. R. Soc. London, Ser. A **253**, 289 (1959).
[25] D. R. Brown, J. Fluid Mech. **10**, 297 (1961).
[26] S. P. Lin and G. Roberts, J. Fluid Mech. **112**, 443 (1981).
[27] S. P. Lin, J. Fluid Mech. **104**, 111 (1981).
[28] D. S. Finnicum, S. J. Weinstein, and K. J. Ruschak, J. Fluid Mech. **255**, 647 (1993).
[29] L. de Luca and M. Costa, J. Fluid Mech. **331**, 127 (1997).
[30] C. H. Teng, S. P. Lin, and J. N. Chen, J. Fluid Mech. **332**, 105 (1997).
[31] L. de Luca, J. Fluid Mech. **399**, 355 (1999).
[32] S. P. Lin, Z. W. Lian, and B. J. Creighton, J. Fluid Mech. **220**, 673 (1990).
[33] P. Luchini, Phys. Fluids **16**, 2154 (2004).
[34] C. Pirat, P. Maissa, and C. Mathis, in *Proceedings of Seventh Rencontres du Non-Linéaire*, edited by Y. Pomeau and R. Ribotta (IHP, Paris, 2004), p. 239.
[35] P. Brunet, C. Clanet, and L. Limat, Phys. Fluids **16**, 2668 (2004).
[36] L. Lebon, L. Limat, P. Brunet, N. Le Grand, and J.-M. Flesselles, in *Proceedings of the Fifth European Coating Symposium*, Fribourg, edited by P. Schweizer (Polytype, Switzerland, 2003).
[37] A. Clarke, S. Weinstein, A. Moon, and E. Simister, Phys. Fluids **9**, 3637 (1997).
[38] P. A. Monkewitz, P. Huerre, and J.-M. Chomaz, J. Fluid Mech. **251**, 1 (1993).
[39] X. Li and R. S. Tankin, J. Fluid Mech. **226**, 425 (1991).
[40] J. S. Roche, N. Le Grand, P. Brunet, L. Lebon, and L. Limat, Phys. Fluids **18**, 082101 (2006).
[41] A movie is available of an entirely subsonic curtain (the Weber number ranges from 0 at the top to 0.6 at the bottom). Although the curtain is perturbed, it stays stable. See http://www.pmmh.espci.fr/~lebon/Subsonic.avi